Conflict Probability and Incrossing Probability in Air Traffic Management

Henk A. P. Blom and G.J. (Bert) Bakker,
National Aerospace Laboratory NLR, Amsterdam, The Netherlands
Email: blom@nlr.nl, bakker@nlr.nl

Abstract
This paper studies performance metrics that are of use in the evaluation of conflict detection and resolution in air traffic management. The metrics studied are conflict probability and incrossing probability, both of which are closely related to the safety criteria used by the civil aviation community. The main contribution of this paper is to develop mathematical characterisations for these metrics, and to show typical differences in their behaviour through numerical evaluations of these metrics for some simple examples.

1 Introduction

In a recent survey, Kuchar and Yang (2000) have shown that there is a large variety of methods that have been proposed in literature to automate Conflict Detection and Resolution (CD&R) in Air Traffic Management (ATM). The survey covered over 60 different CD&R methods, some of which are currently in use under operational evaluation. These methods have been categorised according to a taxonomy that includes: dimension of state information (vertical, horizontal or both); prediction basis (nominal, worst case or probabilistic); conflict detection threshold; conflict resolution method (prescribed, optimised, force field, or manual); manoeuvring dimensions (speed change, lateral, vertical, or combinations); and conflict management (pairwise or global).

Kuchar and Yang (2000) characterises this CD&R development for ATM as one in which a given solution approach to the problem is proposed and exercised, typically through a set of constrained and simplified examples; there has been little crosscutting comparison or synthesis between methods. To improve this situation Kuchar and Yang (2000) recommend the adoption and development of performance-based CD&R design approaches, in which well defined performance metrics allow to make relevant comparisons of a design against the design objectives and against other designs. In support of this approach, the aim of this paper is to contribute to the mathematical characterisation of two performance metrics: conflict probability and incrossing probability. In addition to this we characterise the related metric of overlap probability.

Of these metrics, conflict probability has received most of the attention in literature (e.g. Paielli and Erzberger, 1997, 1999; Prandini et al., 2000). Conflict probability is the probability that the distance between a pair of aircraft becomes smaller than some specified minimum separation value. Paielli and Erzberger's emphasis was on the development of algorithms to numerically evaluate approximations of conflict probabilities. Prandini et al. (2000) emphasized analysis of the problem and clearly distinguished three sub-problems of evaluating conflict probability: 1) to predict the joint density of the aircraft pair considered, 2) to evaluate the instantaneous conflict probability by integrating over the joint density, and 3) to identify the moment in time at which the instantaneous conflict probability reaches its maximum. On this basis, Prandini et al. (2000) developed a randomized optimisation approach for horizontal conflicts, and explained under which type of situations this yields a more accurate assessment than the Paielli and Erzberger (1997) approach does.

The strong point of conflict probability is its clear relation to a well known safety criterion in civil aviation: the separation minimum, which puts a requirement on the air traffic management system not to let aircraft come closer to each other than a certain minimum distance. Depending of the type of airspace and air traffic management, different separation minimum apply (e.g. ICAO, 1998). Moreover such a minimum may come in two forms:

- a minimum on the actual separation
- a minimum on the predicted miss distance

An example of the latter is the 1000 feet minimum difference between flight levels that are allowed to en-route aircraft at the same horizontal position. An example of the former is a 5 Nm minimum horizontal separation between radar controlled en-route aircraft that do not satisfy the vertical separation minimum. Most work on conflict probability has been directed to the latter type of minimum separation.

The overlap probability is the probability that the predicted aircraft physical volumes overlap. Thus, if we would reduce the minimum distance value in conflict probability to about the size of an aircraft, then we arrive approximately at overlap probability.

In addition to minimum separation values, ICAO has also defined limiting criteria for acceptable levels of fatal accident risk, and in particular for the risk of mid air collision (e.g. ICAO, 1998). The allowed probability

This research has been performed with support of the European Commission through the HYBRIDGE project.

values for such events are in the order of one mid-air collision or physical incrossing per 10^9 flight hour. The civil aviation community has also developed a mathematical model to predict these risk values for some basic types of air traffic management. This model is known as the Reich collision model (Reich, 1964). Hsu (1981) has shown that this ICAO adopted Reich model actually keeps on counting any incrossings that follow the first incrossing, which is the collision. Hence it would be better to refer to the Reich incrossing model. In Bakker & Blom (1993) a generalized Reich incrossing model has been developed in order to cover a much larger variety of air traffic situations. For the use of this towards the prediction of incrossings between two aircraft three sub-problems need to be addressed: 1) Prediction of joint probability density functions, 2) Assessment of the incrossing rate, and 3) Integration of the incrossing rate over the time interval considered, and from this the incrossing probability.

The aim of this paper is to develop mathematical characterisations for conflict probability and incrossing probability. In Section 2 the probability density prediction problem is formulated as one of evaluating a weighted sum of Gaussian densities in time. In Section 3, the Incrossing probability is characterised for a Gaussian and a sum of Gaussian densities. In Section 4, the conflict probability is characterised for a Gaussian and a sum of Gaussian densities. In Section 5 another metric, overlap probability, is defined. In Section 6, we compare the metrics through some numerical evaluations for the example considered by Paielli and Erzberger (1997). Section 7 presents concluding remarks.

2 Gaussian sum density

We consider an N-aircraft evolution model that is represented by stochastic differential equations, one for each of the N aircraft, i.e. for $i = 1,\cdots,N$

$$dx_t^i = f^i(x_t, \theta_t, t)\,dt + g^i(x_t, \theta_t, t)\,dw_t^i \qquad (1)$$

with $x_t \equiv \mathrm{Col}\{x_t^1,\cdots,x_t^N\}$, $\theta_t \equiv \mathrm{Col}\{\theta_t^1,\cdots,\theta_t^N\}$, $w_t \equiv \mathrm{Col}\{w_t^1,\cdots,w_t^N\}$, $\{w_t^i\}$ an n-dimensional standard Brownian motion, x^i assumes values in $\mathbb{R}^n$ and θ_t^i a finite state process such that $\{x_t, \theta_t\}$ is a Markov process. The mappings f and g may represent planning and control strategies. Some elements of x_t^i form the 3D position of aircraft i, i.e. $s_t^i = H\,x_t^i$, with H a $3\times n$ matrix.

To avoid Brownian motion behaviour in position, we adopt the assumption

A.1 $\quad H\,g^i(x_t, \theta_t, t) = 0$ for $i = 1,\cdots,N$

Under assumption **A.1**, we get for $i = 1,\cdots,N$

$ds_t^i = v_t^i\,dt$ with $v_t^i \equiv H\,f^i(x_t, \theta_t, t)$.

Next, with s_t^i and s_t^j representing the positions of the centers of aircraft pair (i, j), the relative 3D position is represented by the process $s_t \equiv s_t^i - s_t^j$, and the relative velocity is represented by the process $v_t \equiv v_t^i - v_t^j$. Hence

$$ds_t = v_t\,dt \qquad (2)$$

On the basis of the above model and a given prior joint density $p_{x_{t_0},\theta_{t_0}}(x,\theta)$, it is possible to predict the joint density of s_t and v_t

$p_{s_t,v_t}(s,v)$, $s \in \mathbb{R}^3$, $v \in \mathbb{R}^3$, $t \in (t_0, t_1]$.

In general, this density is not Gaussian, even when it was at t_0. A well known approach from non-linear filtering theory, is to develop an appropriate characterisation of a predicted density $p_{x_t}(x)$ as a Guassian sum density, i.e.

$$p_{x_t}(x) = \sum_l \beta^l(t)\mathrm{N}\left\{x; \mu^l(t), Q^l(t)\right\}$$

with $\beta^l(t) > 0$ for all l and t, such that $\sum_l \beta^l(t) = 1$

and $\mathrm{N}(\cdot, \mu, Q)$ denoting a Gaussian density with mean μ and covariance Q. Similarly, the density $p_{s_t,v_t}(s,v)$ can be represented as a sum of Gaussian densities, i.e.

$$p_{s_t,v_t}(s,v) = \sum_l \beta^l(t)\mathrm{N}\left\{\begin{bmatrix} s \\ v \end{bmatrix}; \begin{bmatrix} \mu_s^l(t) \\ \mu_v^l(t) \end{bmatrix}, \begin{bmatrix} Q_s^l(t) & Q_{s,v}^l(t)^T \\ Q_{s,v}^l(t) & Q_v^l(t) \end{bmatrix}\right\}$$

with $\mu_s^l(t)$, $\mu_v^l(t)$, $Q_s^l(t)$, $Q_v^l(t)$, $Q_{s,v}^l(t)$ the means, covariances and cross-covariance of s_t and v_t given the l-*th* Gaussian in the sum applies.

In view of this Gaussian sum joint density model, the incrossing probability and conflict probability metrics are now characterised for Gaussian and Gaussian sum densities.

3 Incrossing probability P_{in}

One of the safety metrics adopted within the civil aviation community is referred to as the risk of collision between aircraft (e.g. ICAO, 1998). In mathematical terms this metric assumes that the physical shape of each aircraft is a box, and that the incrossing rate of the boxes around these aircraft is integrated over the time period considered (Hsu, 1981).

Generalized Reich model

For processes satisfying (2), Bakker and Blom (1993) have studied the frequency at which the relative position enters a closed area D around the origin, where D consists of a fixed box, the sizes of which add the sizes of two individual aircraft, i.e.

$D \equiv D_1 \times D_2 \times D_3$

with $D_k \equiv [-m_k, m_k]$, $m_k > 0$, $k = 1,2,3$, where m_k denotes the size of one aircraft in k-th direction (for simplicity only m_k is assumed to be aircraft invariant).

If the relative position s_t enters D at time t, i.e. if $s_{t-\Delta} \notin D$ and $s_t \in D$ for $\Delta \downarrow 0$, then we say an incrossing event occurred. For the model we assume that D is transient (non-absorbing). Hence, different from reality, in the model multiple incrossings between aircraft i and j may occur. The incrossing rate at time t is defined as the expected number of incrossings at time t per unit time.

$$\varphi(t) \equiv \lim_{\Delta \downarrow 0} \frac{P\{s_t \in D, s_{t-\Delta} \notin D\}}{\Delta} \qquad (3)$$

and the incrossing integral or incrossing risk $I_{in}(t_0, t_1)$ between two aircraft as the integration of the incrossing rate over a time period $(t_0, t_1]$:

$$I_{in}(t_0, t_1) = \int_{t_0}^{t_1} \varphi(t)\, dt \qquad (4a)$$

Next, the incrossing probability is defined by

$$P_{in}(t_0, t_1) \equiv 1 - \exp\{-I_{in}(t_0, t_1)\} \qquad (4b)$$

Substitution of (4a) into (4b) yields one equation:

$$P_{in}(t_0, t_1) = \int_{t_0}^{t_1} [1 - P_{in}(t_0, t)]\, \varphi(t)\, dt \qquad (5)$$

Under assumption **A.1** and some additional technical conditions, in (Bakker and Blom, 1993, Theorem 1) the following characterisation for incrossing rate has been developed:

$$\varphi(t) = \sum_{k=1}^{3} \int_{\underline{D}_k} \left\{ \int_0^{\infty} v_k\, p_{\underline{s}_{k,t}, s_{k,t}, v_{k,t}}(\underline{s}_k, -m_k, v_k)\, dv_k + \int_{-\infty}^{0} -v_k\, p_{\underline{s}_{k,t}, s_{k,t}, v_{k,t}}(\underline{s}_k, m_k, v_k)\, dv_k \right\} d\underline{s}_k \qquad (6)$$

where

$$\underline{D}_1 \equiv D_2 \times D_3, \quad \underline{D}_2 \equiv D_1 \times D_3, \quad \underline{D}_3 \equiv D_1 \times D_2$$
$$\underline{s}_1 \equiv (s_2, s_3), \quad \underline{s}_2 \equiv (s_1, s_3), \quad \underline{s}_3 \equiv (s_1, s_2)$$

Remark 1: Bakker and Blom (1993) verified that similar equations have been derived by Leadbetter (1966, 1973) and by Marcus (1977) for a one-dimensional process, and by Belyaev (1968) for a multi-dimensional process.

Remark 2: Bakker and Blom (1993; Section 3.4) have shown that under two additional conditions, i.e. if 1) s_t and v_t are independent, and 2) $p_{x_t}(x)$ is constant within D, then eqs. (4a) and (6) are equivalent to the Reich model. Implicitly the Reich model also assumes that D is non-absorbing, and that the orientation of D is not changing dynamically in time.

Remark 3: In reality the first incrossing event is a collision. Hence, the incrossing probability forms an upper bound for the collision probability

$$P_{\text{collision}}(t_0, t_1) \le P_{in}(t_0, t_1)$$

In applications this difference should be kept sufficiently small through an appropriate modelling of aircraft evolution (1).

Gaussian sum case

If the relative position and velocity satisfy a joint Gaussian density, then (6) can be simplified. This is formulated in Theorem 1.

Theorem 1

If conditions hold true under which (6) is satisfied, and $\{s_t, v_t\}$ is Gaussian with means $\mu_s(t)$, $\mu_v(t)$ and covariances $Q_s(t)$, $Q_v(t)$ and $Q_{s,v}(t)$, then the incrossing rate satisfies:

$$\varphi(t) = \sum_{k=1}^{3} \int_{\underline{D}_k} [\nu_k^+(\underline{s}_k, -m_k, t)\, p_{\underline{s}_{k,t}, s_{k,t}}(\underline{s}_k, -m_k) + \nu_k^-(\underline{s}_k, m_k, t)\, p_{\underline{s}_{k,t}, s_{k,t}}(\underline{s}_k, m_k)]\, d\underline{s}_k \qquad (7a)$$

$$\nu_k^+(s,t) = \frac{e^{-a_k(t) d_k^2(s,t)}}{\sqrt{4\pi |a_k(t)|}} + \frac{1}{2} d_k(s,t)\left[1 + \mathrm{Erf}(d_k(s,t)\sqrt{a_k(t)})\right], \; s \in \mathbb{R}^3 \qquad (7b)$$

$$\nu_k^-(s,t) = \frac{e^{-a_k(t) d_k^2(s,t)}}{\sqrt{4\pi |a_k(t)|}} - \frac{1}{2} d_k(s,t)\left[1 - \mathrm{Erf}(d_k(s,t)\sqrt{a_k(t)})\right], \; s \in \mathbb{R}^3 \qquad (7c)$$

with $\underline{D}_k$, D_k, $\underline{s}_k$ and s_k as in (6) and

$$a_k(t) = \frac{1}{2}[Q_{v_k}(t) - Q_{s,v_k}(t)^T Q_s^{-1}(t) Q_{s,v_k}(t)]^{-1}$$
$$d_k(s', t) = \mu_{v_k}(t) + Q_{s,v_k}(t)^T Q_s^{-1}(t)(s' - \mu_s(t))$$

where $\mu_{v_k}(t)$ is the k-th element of $\mu_v(t)$, $Q_{v_k}(t)$ is the k-th diagonal element of $Q_v(t)$, and $Q_{s,v_k}(t)$ is the k-th column of $Q_{s,v}(t)$.

Proof: See appendix A.

Corollary 1: If at time t the relative position and velocity satisfy a Gaussian sum density with weights $\beta^l(t)$, then

$$\varphi(t) = \sum_l \beta^l(t)\, \varphi^l(t)$$

where $\varphi^l(t)$ satisfies Theorem 1 for each l.

Remark 4: For many applications, numerical evaluations of the incrossing probability need a limited precision (e.g. 1%). Then it is often sufficient to adopt a first order approximation for the integrals in (5) and (7):

$$P_{in}(t_0, t_1) \approx \int_{t_0}^{t_1} \varphi(t)\, dt$$

$$\varphi(t) \approx 4 m_1 m_2 m_3 \sum_{k=1}^{3} \frac{1}{m_k} \cdot \left[\nu_k^+(0, -m_k, t)\, p_{\underline{s}_{k,t}, s_{k,t}}(0, -m_k) + \nu_k^-(0, m_k, t)\, p_{\underline{s}_{k,t}, s_{k,t}}(0, m_k)\right]$$

4 Conflict Probability P_c

In (Prandini et al., 2000) the instantaneous probability of a horizontal conflict at time t is defined as the probability that at time t two aircraft that fly at the same vertical position (i.e. $s_{\perp,t} = 0$), will be within a conflict distance d from one another. If we introduce a diagonal matrix $S = \text{diag}\{1, 1, \alpha_\perp\}$, with $\alpha_\perp \geq 1$ an appropriate relative vertical position scaling factor, then the instantaneous probability of conflict, $P_{ic}(t)$, at time t is given by:

$$P_{ic}(t) \equiv \text{Prob}\{\| S\, s_t \| \leq \text{d}\} = \iint_{\|S\, s\| \leq \text{d}} p_{s_t}(s)\, ds \qquad (8)$$

where $p_{s_t}(s)$ is the predicted probability density function of the relative position s_t at time t. The probability of conflict in time interval $(t_0, t_1]$ is then given by

$$P_c(t_0, t_1) \equiv \max_{t \in [t_0, t_1]} P_{ic}(t), \quad \text{if} \quad s_{\perp,t} = 0 \quad \text{for} \quad t \in [t_0, t_1].$$

Gaussian sum case

If the predicted relative horizontal position s_t' is Gaussian and if the predicted relative vertical position $s_{\perp,t} = 0$ and we make use of the error function

$$\text{Erf}(x) \equiv \frac{2}{\sqrt{\pi}} \int_0^x e^{-z^2} dz$$

then $P_{ic}(t)$ can be characterised as follows.

<u>Theorem 2</u>

When the predicted relative vertical position $s_{\perp,t} = 0$, and the predicted relative horizontal position s_t' is Gaussian, with mean $\mu_s'(t)$ and positive definite covariance $Q_s'(t)$, then $P_{ic}(t)$ satisfies:

$$P_{ic}(t) = \int_{\bar{y}_2(t)-d}^{\bar{y}_2(t)+d} \left[\frac{1}{2} \left\{ \text{Erf}\left(\frac{\bar{y}_1(t) + g(y_2, \bar{y}_2(t), d)}{\sqrt{2\lambda_1(t)}} \right) - \text{Erf}\left(\frac{\bar{y}_1(t) - g(y_2, \bar{y}_2(t), d)}{\sqrt{2\lambda_1(t)}} \right) \right\} \cdot \frac{e^{-\frac{1}{2}\frac{y_2^2}{\lambda_2(t)}}}{\sqrt{2\pi\lambda_2(t)}} \right] dy_2 \qquad (9)$$

with

$$g(y_2, \bar{y}_2, d) = \sqrt{d^2 - (y_2 - \bar{y}_2)^2}$$

$$\text{Col}\{\bar{y}_1(t), \bar{y}_2(t)\} = -R(t)\,\mu_s'(t)$$

$$\text{Diag}\,(\lambda_1(t), \lambda_2(t)) = R(t) Q_s'(t) R(t)^T$$

where $R(t)$ is a 2×2 rotation matrix (i.e. $R(t)^T = R(t)^{-1}$) such that $R(t)\, Q_s'(t)\, R(t)^T$ is a diagonal matrix.

<u>Proof:</u> See appendix B.

<u>Corollary 2</u>: If at time t the relative position and velocity satisfy a sum of Gaussian densities with weights $\beta^l(t)$ then

$$P_{ic}(t) = \sum_l \beta^l(t) P_{ic}^l(t)$$

where $P_{ic}^l(t)$ satisfies Theorem 2 for each l.

5 Overlap probability P_o

The overlap probability over the interval $(t_o, t_1]$ is defined in terms of the closed area D as follows

$$P_o(t_0, t_1) \equiv \max_{t \in [t_0, t_1]} P_{io}(t)$$

with $P_{io}(t)$ the instantaneous overlap probability satisfying

$$P_{io}(t) \equiv P(s_t \in D) = \int_D p_{s_t}(s) ds \qquad (10)$$

Although the overlap probability considers the same closed area D as the incrossing integral does, there is a significant difference between incrossing integral and overlap probability. In Appendix C it is shown that

$$I_{in}(t_0, t_1) = P_o(t_0, t_1) - P_{io}(t_0) + I_{out}(t_0, \tau) + I_{in}(\tau, t_1)$$

with $\tau \equiv \arg\max_{t \in [t_0, t_1]} P_{io}(t)$, and with $I_{out}(t_0, \tau)$ the D-outcrossing integral over $(t_0, \tau]$.

In words this means: if two aircraft are separated at t_0, then the incrossing integral over $(t_0, t_1]$ is equal to the sum of the following three non-negative terms

1. The overlap probability $P_o(t_0, t_1)$ over $(t_0, t_1]$.
2. The incrossing integral $I_{in}(\tau, t_1)$ over $(\tau, t_1]$.
3. The outcrossing integral $I_{out}(t_0, \tau)$ over $(t_0, \tau]$.

6 Numerical example

In the sequel, the incrossing probability, the conflict probability and the overlap probability metrics are numerically evaluated and compared by applying them to the linear Gaussian example considered by Paielli and Erzberger (1997). In this example two aircraft paths cross each other at the same flight level. Four scenarios (see Table 1) are evaluated on P_{in}, P_c, P_o and the conflict probability approach of Paielli & Erzberger (1997). The results are shown in Figures 1 through 3.

Table 1 Scenarios 1-4 and their parameter values. The scenario variables are:(a.) predicted miss distance, (b.) path crossing angle, (c.) predicted ground speeds, (d.) time before predicted miss, (e.) growth-rate of along-track standard deviation (s.d.), (f) across-track standard deviation. The along-track s.d. at predicted miss follows from the product of d. and e.

Parameter	Scen 1	Scen 2	Scen 3	Scen 4
a. [Nm]	6	4	6	6
b. [deg]	90	90	10-180	10-180
c. [kts]	480	480	480 behind 420	480 before 420
d. [min]	1-40	1-40	4	4
e. [kts]	15	15	10	10
f. [Nm]	1	1	1	1

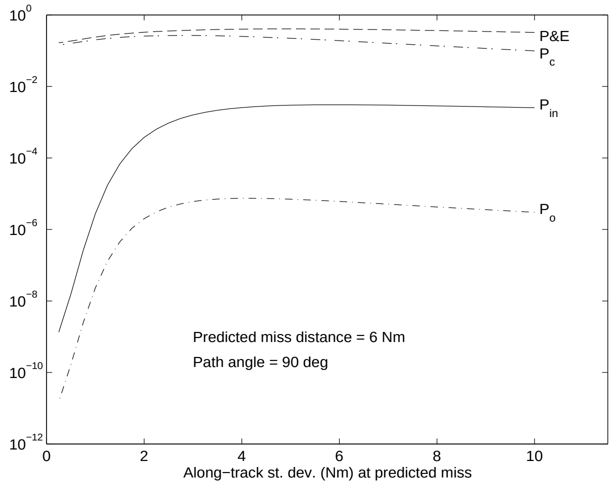

Figure 1 Conflict probability, overlap probability and incrossing probability for scenario 1).*

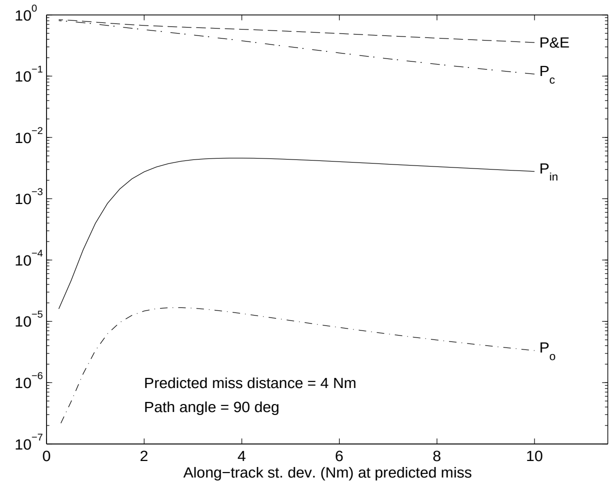

Figure 2 Conflict probability, overlap probability and incrossing probability for scenario 2).*

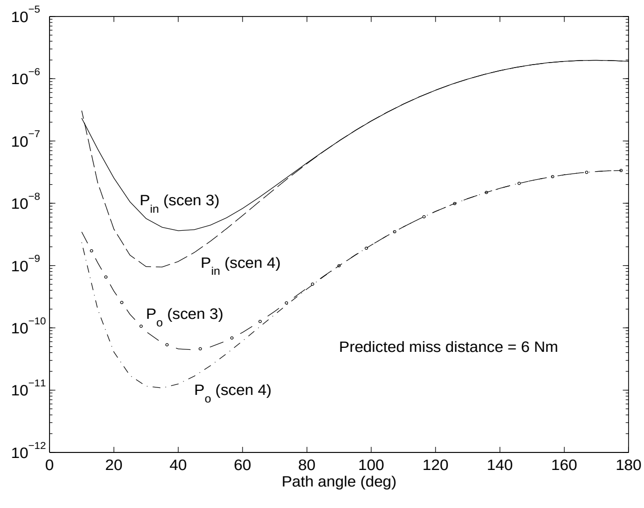

Figure 3 Difference between scenarios 3 and 4; faster aircraft crosses behind and before slower aircraft).*

Paielli & Erzberger versus conflict probability P_c

Figures 1 and 2 clearly show that in general the P&E algorithm does not provide an accurate assessment of conflict probability. In figures 1 and 2 the error increases with increasing uncertainty, up to a factor 4. Paielli & Erzberger (1997) already concluded that for this example conflict probabilities for predicted miss distances below 5 Nm behave differently than for predicted miss distances above 5 Nm. If the predicted miss distance is larger than 5 Nm, Figure 1 illustrates the typical behavior of the conflict probabilities; first with increasing along-track position uncertainty from zero, the conflict probability increases from zero to a maximum and then it decreases again.

Overlap probability P_o versus conflict probability P_c

In Figure 1 it can be seen that for large uncertainties in the along-track position the conflict probability and the overlap probability are approximately equally sensitive to changes in the uncertainty. Thus for situations in which large uncertainties are common, both probabilistic approaches can be used. A good example, is flow management. However, if the uncertainties in along-track position become smaller, overlap probability is much more sensitive to changes in along-track uncertainty than conflict probability. When in Figure 1 the uncertainty in the along-track position decreases, the overlap probability values decrease very fast to very small values, where conflict probability values hardly decrease. So in this example, when aircraft get closer to the point of predicted miss, the more sensitive overlap probability becomes in comparison to conflict probability. For small uncertainties this means overlap probability better allows to distinguish between safe and unsafe situations than conflict probability. If the predicted miss distance is smaller than 5 Nm, with increasing along-track position uncertainty from zero, the conflict probability steadily decreases from its maximum towards zero. For incrossing probability and overlap probability such a distinction is not necessary as can be seen from Figures 1 and 2. For a predicted miss distance of 4 Nm and 6 Nm, with decreasing along-track position uncertainties, the incrossing probability and overlap probability slowly increase to a certain maximum and then decrease to very small values. This means that conflict probability can give no information with regard to the possible modifications of separation minima, where incrossing probability can.

Incrossing probability P_{in} versus overlap probability P_o

The faster the aircraft fly, the shorter the encounter or period of potential conflict will be, while the larger relative speed enlarges the incrossing rate during the period of encounter or possible conflict. The consequence of the smaller time period is a potential reduction of incrossing probability, where the larger speed difference increases the incrossing probability. Thus incrossing probability always

*) Because of computer coding error correction, the numerical results differ from those in Bakker et al. (2001)

shows a trade-off between these two effects, while overlap probability (and conflict probability) won't. In Figures 1 through 3 the ratio between P_{in} and P_o varies from a factor 55 up to a factor 830. Hence it can be concluded that in this example, the above trade-off is such that the two consequences do not balance. A clear advantage of incrossing probability over overlap probability is that the former is an ICAO adopted ATM safety metric, and the latter is not.

7 Concluding remarks

For the development of performance-based CD&R design approaches in ATM, well defined performance metrics are needed to make relevant comparison of a design against the design objectives and against other designs. In support of such approach, this paper has studied the safety related performance metrics: conflict probability, incrossing probability and overlap probability. For these metrics novel mathematical characterisations have been developed and the relation with previous work has been explained. Subsequently, the novel characterisations have been used to numerically evaluate some simple aircraft crossing scenarios and to compare the results obtained for the different metrics. For the scenarios considered the overlap and incrossing probability metrics appeared to respond most meaningful to changes in the conflict scenario parameters. The specific advantage of incrossing probability over overlap probability is that the former an ICAO adopted ATM safety metric. A disadvantage is that the numerical evaluation of incrossing probability is more demanding. For performance evaluation purposes, however, this is not a critical issue. For other illustrative applications of the incrossing probability metric see:

- Accident risk assessment of air traffic operations (Blom et al., 2001a, 2001b).
- Modelling of conflict detection in CD&R (Van Doorn et al, 2001).

Acknowledgement: The authors would like to thank John Lygeros (Univ. of Cambridge, UK), Xanthi Papageorgiou (PhD student at National Technical Univ. of Athens) and an anonymous reviewer for valuable comments.

8 References

Kuchar, J.K. and L.C. Yang, A review of conflcit detection and resolution modeling methods, IEEE Tr. on Intelligent Transportation Systems, Vol. 1, No. 4, 2000, pp. 179-189.

Prandini, M., J. Hu, J. Lygeros and S. Sastry, A probabilistic approach to aircraft conflict detection, IEEE Tr. on Intelligent Transportation Systems, Vol. 1, No. 4, 2000, pp. 199-220.

Paielli, R.A. and H. Erzberger, "Conflict probability estimation for free flight", AIAA J. of Guidance, Control and Dynamics, Vol. 20, 1997, pp.588-596.

Paielli, R.A. and H. Erzberger, "Conflict Probability Estimation Generalised to Non-Level Flight", Air Traffic Control Quarterly, Vol. 7, pp.195-222, 1999.

ICAO, *Annex 11 – Air Traffic Services*, 12th edition, incorporating amendments 1-38, July 1998, Green pages, attachment B, paragraph 3.2.1.

Reich, P.G., "A theory of safe separation standards for Air Traffic Control", Technical report 64041, Royal Aircraft Establishment, U.K., 1964.

Hsu, D.A., "The evaluation of aircraft collision probabilities at intersecting air routes", J. of Navigation, Vol.34 (1981), pp.78-102.

Bakker, G.J. and H.A.P. Blom, "Air traffic collision risk modelling". Proc. 32nd IEEE Conf. on Decision and Control, pp. 1464-1469, 1993. (NLR Report TP93292 includes the proofs of the theorems).

Leadbetter, M.R., "On crossing of levels and curves by a wide class of stochastic processes", Ann. Math. Statist., Vol. 37, pp. 260-267, 1966.

Leadbetter, M.R., "Point processes generated by level crossings", in Stochastic Point Processes, Ed. P. Lewis, Wiley, New York, 1973.

Marcus, M.B., "Level crossings of a stochastic process with absolutely continuous sample paths", The Annuals of Probability, Vol. 5, pp. 52-71, 1977.

Belyaev, Y.K., "On the number of exits across the boundary of a region by a vector stochastic process", Theory Probab. Appl, Vol 13, pp. 320-324, 1968.

Blom, H.A.P., G.J. Bakker, P.J.G. Blanker, J. Daams, M.H.C. Everdij and M.B. Klompstra, Accident Risk Assessment for Advanced Air Traffic Management. Eds: G.L. Donohue and A.G. Zellweger, Air Transportation Systems Engineering, AIAA, pp. 463-480, 2001a.

Blom, H.A.P., M.B. Klompstra, G.J. Bakker,, Accident risk assessment of Simultaneous Converging Instrument Approaches, Proc. 4th USA/Europe ATM R&D Seminar, Santa Fe, December 2001b. http://atm2001.eurocontrol.fr/

Bakker, G.J., H.J. Kremer and H.A.P. Blom, Probabilistic Approaches Toward Conflict Prediction. Eds: G.L. Donohue and A.G. Zellweger, Air Transportation Systems Engineering, AIAA, pp. 677-694, 2001.

Van Doorn, B.A., G.J. Bakker, C. Meckiff, Evaluation of Advanced Conflict Modelling using the Highly Interactive Problem Solver, Proc. 4th USA/Europe ATM R&D Seminar, Santa Fe, December 2001. http://atm2001.eurocontrol.fr/

Kremer, H.J. and G.J. Bakker, A probabilistic approach towards conflict probing, NLR report TR 97041 L, 1997

Gradshteyn, I.S., I.M. Ryzhik, "Table of integrals, series and products", Academic Press, New York, 1980.

Strang, G., Linear algebra and its applications, Academic Press, New York, 1980.

Appendix A Proof of Theorem 1

The proof of Theorem 1 is based on Kremer and Bakker (1997). First two Lemma's are introduced.

Lemma 1

For a>0:

$$\int_0^\infty v e^{-a(v-d)^2} dv = \left(e^{-ad^2} + d\sqrt{\pi a}(1+\mathrm{Erf}(d\sqrt{a}))\right)\frac{1}{2a}$$

Proof According to Gradshteyn & Ryzhik (1980; equation 3.462.5)

$$\int_0^\infty v e^{-av^2-2bv} dv = \left(1 - b\sqrt{\frac{\pi}{a}}\, e^{\frac{b^2}{a}}(1-\mathrm{Erf}(\frac{b}{\sqrt{a}}))\right)\frac{1}{2a}$$

with $\mathrm{Erf}(x) = \frac{2}{\sqrt{\pi}}\int_0^x e^{-z^2}dz$

Hence,

$$\int_0^\infty ve^{-a(v-d)^2}dv = e^{-ad^2}\int_0^\infty ve^{-av^2+2adv}dv$$

$$= e^{-ad^2}\left(1+ad\sqrt{\frac{\pi}{a}}\,e^{\frac{(-ad)^2}{a}}(1-\mathrm{Erf}(\frac{-ad}{\sqrt a}))\right)\frac{1}{2a}$$

$$= e^{-ad^2}\left(1+d\sqrt{\pi a}\, e^{ad^2}(1+\mathrm{Erf}(d\sqrt a))\right)\frac{1}{2a}$$

$$= \left(e^{-ad^2}+d\sqrt{\pi a}(1+\mathrm{Erf}(d\sqrt a))\right)\frac{1}{2a} \qquad \square$$

Lemma 2

If we define

$$v_k^+(s,t) \equiv \int_0^\infty v\, p_{v_{k,t}|s_t}(v,s)dv \qquad \text{(A.1)}$$

$$v_k^-(s,t) \equiv \int_{-\infty}^0 -v\, p_{v_{k,t}|s_t}(v,s)dv \qquad \text{(A.2)}$$

Then

$$v_k^+(s,t) = \frac{e^{-a_k(t)d_k^2(s,t)}}{2\sqrt{\pi\,|\,a_k(t)\,|}} + \frac12 d_k(s,t)[1+\mathrm{Erf}(d_k(s,t)\sqrt{a_k}(t))]$$

and

$$v_k^-(s,t) = \frac{e^{-a_k(t)d_k^2(s,t)}}{2\sqrt{\pi\,|\,a_k(t)\,|}} - \frac12 d_k(s,t)[1-\mathrm{Erf}(d_k(s,t)\sqrt{a_k}(t))]$$ with

$$a_k(t) \equiv \frac12[Q_{v_k}(t) - Q^T_{s,v_k}(t)Q_s^{-1}(t)Q_{s,v_k}(t)]^{-1}$$

and $d_k(s',t) \equiv \mu_{v_k}(t) + Q^T_{s,v_k}(t)Q_s^{-1}(t)(s'-\mu_s(t))$.

Proof Since s_t and $v_{k,t}$ are jointly Gaussian we can show

$$E\{v_{k,t}\,|\,s_t=s'\} = \mu_{v_k}(t)+Q^T_{sv_k}(t)Q_s^{-1}(t)(s'-\mu_s(t))$$

$$E\{[\bar v_k(s',t)-v_{k,t}]^2\,|\,s_t=s'\} = Q_{v_k}(t)-Q^T_{sv_k}(t)Q_s^{-1}(t)Q_{sv_k}(t)$$

Using this for $p_{v_{k,t}|s_t}(v,s)$ in (A.1) yields:

$$v_k^+(s,t) = \frac{1}{\sqrt{\pi\,|\,a_k^{-1}(t)\,|}}\int_0^\infty ve^{-a_k(t)[v-d_k(s,t)]^2}dv$$

Now Lemma 1 is used to get (for simplicity arguments s and t are left out):

$$v_k^+ = \frac{1}{\sqrt{\pi\,|\,a_k^{-1}\,|}}\left(e^{-a_kd_k^2}+d_k\sqrt{\pi a_k}(1+\mathrm{Erf}(d_k\sqrt{a_k}))\right)\frac{1}{2a_k}$$

$$= \frac{1}{2\sqrt{\pi\,|\,a_k\,|}}e^{-a_kd_k^2}+\frac12 d_k(1+\mathrm{Erf}(d_k\sqrt{a_k}))$$

A similar approach applied to (A.2) for $v_k^-(s,t)$ yields:

$$v_k^-(s,t) = \frac{1}{\sqrt{\pi\,|\,a_k^{-1}(t)\,|}}\int_0^\infty ve^{-a_k(t)[v+d_k(s,t)]^2}dv$$

Subsequently, Lemma 1 yields:

$$v_k^- = \frac{1}{\sqrt{\pi\,|\,a_k^{-1}\,|}}.\left(e^{-a_kd_k^2}-d_k\sqrt{\pi a_k}(1+\mathrm{Erf}(-d_k\sqrt{a_k}))\right)\frac{1}{2a_k}$$

$$= \frac{1}{2\sqrt{\pi\,|\,a_k\,|}}e^{-a_kd_k^2}-\frac12 d_k(1-\mathrm{Erf}(d_k\sqrt{a_k})) \qquad \square$$

On the basis of this we prove Theorem 1.

Proof of Theorem 1

From Bakker and Blom (1993; Theorem 1), the incrossing rate satisfies:

$$\varphi(t) = \sum_{k=1}^3\int_{\underline D_k}\left\{\int_0^\infty v_k\, p_{\underline s_{k,t},s_{k,t},v_{k,t}}(\underline s_k,-m_k,v_k)dv_k + \int_{-\infty}^0 -v_k\, p_{\underline s_{k,t},s_{k,t},v_{k,t}}(\underline s_k,m_k,v_k)dv_k\right\}d\underline s_k$$

Straightforward conditioning yields:

$$\varphi(t) = \sum_{k=1}^3\int_{\underline D_k}\left\{\int_0^\infty v_k\, p_{v_{k,t}|\underline s_{k,t},s_{k,t}}(v_k,\underline s_k,-m_k)\,p_{\underline s_{k,t},s_{k,t}}(\underline s_k,-m_k)dv_k + \int_{-\infty}^0 -v_k\, p_{v_{k,t}|\underline s_{k,t},s_{k,t}}(v_k,\underline s_k,m_k)\,p_{\underline s_{k,t},s_{k,t}}(\underline s_k,m_k)dv_k\right\}d\underline s_k$$

$$= \sum_{k=1}^3\int_{\underline D_k}\left\{\int_0^\infty v_k\, p_{v_{k,t}|\underline s_{k,t},s_{k,t}}(v_k,\underline s_k,-m_k)\,dv_k\;\, p_{\underline s_{k,t},s_{k,t}}(\underline s_k,-m_k) + \int_{-\infty}^0 -v_k\, p_{v_{k,t}|\underline s_{k,t},s_{k,t}}(v_k,\underline s_k,m_k)\,dv_k\;\, p_{\underline s_{k,t},s_{k,t}}(\underline s_k,m_k)\right\}d\underline s_k$$

Together with Lemma 2 this yields eq. (7):

$$\varphi(t) = \sum_{k=1}^{3} \int_{\underline{D}_k} [\, \nu_k^+(\underline{s}_k, -m_k, t)\, p_{\underline{s}_{k,t}, s_{k,t}}(\underline{s}_k, -m_k) + $$
$$+ \nu_k^-(\underline{s}_k, m_k, t)\, p_{\underline{s}_{k,t}, s_{k,t}}(\underline{s}_k, m_k)]\ d\,\underline{s}_k \qquad \square$$

Appendix B Proof of Theorem 2

First two Lemma's are introduced.

Lemma 3

$$\int_0^x \frac{e^{-\frac{1}{2}\frac{y^2}{\lambda}}}{\sqrt{2\pi\lambda}}\, dy = \frac{1}{2}\,\mathrm{Erf}\left(\frac{x}{\sqrt{2\lambda}}\right), \qquad \lambda > 0$$

Proof The Erf(.) is defined as (e.g. Gradshteyn & Ryzhik, 1980 p. xxxiv) :

$$\mathrm{Erf}\,(x) \equiv \frac{2}{\sqrt{\pi}} \int_0^x e^{-z^2}\, dz$$

Integrating w.r.t. $y = z\sqrt{2\lambda}$ yields

$$\mathrm{Erf}\,(x) = \sqrt{\frac{2}{\pi\lambda}} \int_0^{\sqrt{2\lambda}\ x} e^{-\frac{1}{2}\frac{y^2}{\lambda}}\, dy \qquad \square$$

Lemma 4

If a matrix Q is real, symmetric and positive definite then the eigenvalues of Q are positive and Q is diagonalizable through a rotation matrix i.e.

$$R\,Q\,R^T = \mathrm{diag}(\mathrm{eigenvalues}(Q)) \equiv \Lambda$$

with R a rotation matrix (i.e. $R^T = R^{-1}$), $Q^{-1} = R^T\,\Lambda^{-1}\,R$ and Det (Q) = Det (Λ).

Proof This is well known from Linear Algebra (see for example Strang, 1980). $\square$

Next, we continue with the proof of Theorem 2 for $s_{\perp,t} = 0$. By definition:

$$P_{ic}(t) = \iint_{\|s'\|^2 \le d^2} \frac{e^{-\frac{1}{2}(s'-\mu_s'(t))^T (Q_s'(t))^{-1} (s'-\mu_s'(t))}}{2\pi\sqrt{Det\,(Q_s'(t))}}\, ds' \qquad \text{(B.1)}$$

Since Lemma 4 applies to the 2×2 matrix $Q_s'(t)$, we have a rotation matrix $R(t)$ such that

$$R(t)Q_s'(t)R(t)^T = \mathrm{diag}(\lambda_1(t), \lambda_2(t)) \equiv \Lambda(t)$$

with $R(t)^T = R(t)^{-1}$ and $\lambda_1(t), \lambda_2(t)$ both positive.

Hence,

$$|\mathrm{Det}(R(t))| = 1,\ \mathrm{Det}(\Lambda(t)) = \mathrm{Det}(Q_s'(t)) = \lambda_1(t)\,\lambda_2(t) \qquad \text{(B.2)}$$

Next define the transformation

$$y \equiv R(t)(s' - \mu_s'(t)) \qquad \text{(B.3)}$$

Then we get

$$dy = R(t)ds' \qquad \text{(B.4)}$$

$$(s'-\mu_s'(t))^T (Q_s'(t))^{-1} (s'-\mu_s'(t)) =$$
$$= (s'-\mu_s'(t))^T R(t)^T \Lambda(t)^{-1} R(t)(s'-\mu_s'(t)) = y^T \Lambda(t)^{-1} y \qquad \text{(B.5)}$$

and

$$\|s'\| = s'^T\ s' = s^T R(t)^T\ R(t)s' = (y + R(t)\mu_s'(t))^T\ (y + R(t)\mu_s'(t)) =$$
$$= (y - \bar{y}(t))^T\ (y - \bar{y}(t)) = \|y - \bar{y}(t)\| \qquad \text{(B.6)}$$

with

$$\bar{y}(t) \equiv -R(t)\,\mu_s'(t) \qquad \text{(B.7)}$$

Further evaluation of (B.1) through integration w.r.t. y and using (B.2-B.7), we get

$$P_{ic}(t) = \iint_{\|y-\bar{y}(t)\|^2 \le d^2} \frac{e^{-\frac{1}{2}y^T\Lambda(t)^{-1}y}}{2\pi\sqrt{Det(\Lambda(t))}}\, dy$$

$$= \int_{-\infty}^{\infty}\int_{-\infty}^{\infty} 1\left\{(y_1 - \bar{y}_1(t))^2 + (y_2 - \bar{y}_2(t))^2 \le d^2\right\} \frac{e^{-\frac{1}{2}y^T\Lambda(t)^{-1}y}}{2\pi\sqrt{Det(\Lambda(t))}}\, dy_1 dy_2$$

$$= \int_{-\infty}^{\infty}\int_{-\infty}^{\infty} 1\left\{-\sqrt{d^2 - (y_2 - \bar{y}_2(t))^2} \le y_1 - \bar{y}_1(t) \le \sqrt{d^2 - (y_2 - \bar{y}_2(t))^2}\right\} \bullet$$
$$\bullet 1\left\{(y_2 - \bar{y}_2(t))^2 \le d^2\right\} \frac{e^{-\frac{1}{2}y^T\Lambda(t)^{-1}y}}{2\pi\sqrt{Det(\Lambda(t))}}\, dy_1\, dy_2$$

$$= \int_{-\infty}^{\infty}\int_{-\infty}^{\infty} 1\{-g(y_2, \bar{y}_2(t), d) \le y_1 - \bar{y}_1(t) \le g(y_2, \bar{y}_2(t), d)\} \bullet$$
$$\bullet 1\{-d \le y_2 - \bar{y}_2(t) \le d\} \frac{e^{-\frac{1}{2}y^T\Lambda(t)^{-1}y}}{2\pi\sqrt{Det(\Lambda(t))}}\, dy_1\, dy_2$$

with $g(y_2, \bar{y}_2, d) = \sqrt{d^2 - (y_2 - \bar{y}_2)^2}$

Further evaluation yields

$$P_{ic}(t) = \int_{\bar{y}_2(t)-d}^{\bar{y}_2(t)+d} \int_{\bar{y}_1(t)-g(y_2,\bar{y}_2(t),d)}^{\bar{y}_1(t)+g(y_2,\bar{y}_2(t),d)} \frac{e^{-\frac{1}{2}y^T\Lambda(t)^{-1}y}}{2\pi\sqrt{Det(\Lambda(t))}}\, dy_1\, dy_2$$

$$= \int_{\bar{y}_2(t)-d}^{\bar{y}_2(t)+d} \int_{\bar{y}_1(t)-g(y_2,\bar{y}_2(t),d)}^{\bar{y}_1(t)+g(y_2,\bar{y}_2(t),d)} \frac{e^{-\frac{1}{2}\left(\frac{y_1^2}{\lambda_1(t)} + \frac{y_2^2}{\lambda_2(t)}\right)}}{2\pi\sqrt{\lambda_1(t)\lambda_2(t)}}\, dy_1\, dy_2$$

$$= \int_{\bar{y}_2(t)-d}^{\bar{y}_2(t)+d} \left[\int_{\bar{y}_1(t)-g(y_2,\bar{y}_2(t),d)}^{\bar{y}_1(t)+g(y_2,\bar{y}_2(t),d)} \frac{e^{-\frac{1}{2}\frac{y_1^2}{\lambda_1(t)}}}{\sqrt{2\pi\lambda_1(t)}}\, dy_1 \right] \frac{e^{-\frac{1}{2}\frac{y_2^2}{\lambda_2(t)}}}{\sqrt{2\pi\lambda_2(t)}}\, dy_2$$

$$= \int_{\bar{y}_2(t)-d}^{\bar{y}_2(t)+d} \left[\int_{0}^{\bar{y}_1(t)+g(y_2,\bar{y}_2(t),d)} \frac{e^{-\frac{1}{2}\frac{y_1^2}{\lambda_1(t)}}}{\sqrt{2\pi\lambda_1(t)}}\, dy_1 \right.$$
$$\left. - \int_{0}^{\bar{y}_1(t)-g(y_2,\bar{y}_2(t),d)} \frac{e^{-\frac{1}{2}\frac{y_1^2}{\lambda_1(t)}}}{\sqrt{2\pi\lambda_{1(t)}}}\, dy_1 \right] \bullet \frac{e^{-\frac{1}{2}\frac{y_2^2}{\lambda_2(t)}}}{\sqrt{2\pi\lambda_2(t)}}\, dy_2$$

Using Lemma 3 this yields :

$$P_{ic}(t)=\int_{\bar{y}_2(t)-d}^{\bar{y}_2(t)+d}[\frac{1}{2}\left\{\mathrm{Erf}\left(\frac{\bar{y}_1(t)+g(y_2,\bar{y}_2(t),d)}{\sqrt{2\lambda_1(t)}}\right)-\mathrm{Erf}\left(\frac{\bar{y}_1(t)-g(y_2,\bar{y}_2(t),d)}{\sqrt{2\lambda_1(t)}}\right)\right\}\cdot$$

$$\cdot\frac{e^{-\frac{1}{2}\frac{y_2{}^2}{\lambda_2(t)}}}{\sqrt{2\pi\lambda_2(t)}}]\,dy_2$$ □

Appendix C. Overlap probability

Proposition 1

$$\frac{\partial P_{io}(t)}{\partial t}=\varphi(t)-\psi(t)$$

with $\varphi(t)$ the incrossing rate defined in (4), and with $\psi(t)$ the outcrossing rate

$$\psi(t)\equiv\lim_{\Delta\downarrow 0}\frac{P(s_t\notin D\ \ ,s_{t-\Delta}\in D)}{\Delta} \qquad \text{(C.1)}$$

Proof: By definition we have

$$\frac{\partial P_{io}(t)}{\partial t}=\lim_{\Delta\downarrow 0}\frac{P_{io}(t)-P_{io}(t-\Delta)}{\Delta}$$

Using (10), we get

$$P_{io}(t)-P_{io}(t-\Delta)=P(s_t\in D)-P(s_{t-\Delta}\in D)=$$
$$=P(s_t\in D,s_{t-\Delta}\notin D)+P(s_t\in D,s_{t-\Delta}\in D)$$
$$-P(s_t\notin D,s_{t-\Delta}\in D)-P(s_t\in D,s_{t-\Delta}\in D)$$
$$=P(s_t\in D,s_{t-\Delta}\notin D)-P(s_t\notin D,s_{t-\Delta}\in D)$$

Substituting this yields

$$\frac{\partial P_{io}(t)}{\partial t}=\lim_{\Delta\downarrow 0}\frac{P(s_t\in D,s_{t-\Delta}\notin D)-P(s_t\notin D,s_{t-\Delta}\in D)}{\Delta}$$

Next using (4) and (C.1) yields:

$$\frac{\partial P_{io}(t)}{\partial t}=\varphi(t)-\psi(t)$$ □

Proposition 2

For $\forall\tau\in[t_0,t_1]$:

$$I_{in}(t_0,t_1)=P_{io}(\tau)-P_{io}(t_0)+\int_{t_0}^{\tau}\psi(t)\,dt+I_{in}(\tau,t_1) \qquad \text{(C.2)}$$

Proof: For any τ assuming values in (t_0, t_1] we have:

$$I_{in}(t_0,t_1)=\int_{t_0}^{t_1}\varphi(t)\,dt=\int_{t_0}^{\tau}\varphi(t)\,dt+\int_{\tau}^{t_1}\varphi(t)\,dt$$

Using Proposition 1 this yields

$$I_{in}(t_0,t_1)=\int_{t_0}^{\tau}[\frac{\partial P_{io}(t)}{\partial t}+\psi(t)]\,dt+\int_{\tau}^{t_1}\varphi(t)\,dt=$$

$$=P_{io}(\tau)-P_{io}(t_0)+\int_{t_0}^{\tau}\psi(t)\,dt+\int_{\tau}^{t_1}\varphi(t)\,dt$$ □

Corollary 4:

If we define $\tau\equiv\arg\max_{t\in[t_0,t_1]}P_{io}(t)$, then (C.2) yields

$$I_{in}(t_0,t_1)=P_o(t_0,t_1)-P_{io}(t_0)+I_{out}(t_0,\tau)+I_{in}(\tau,t_1)$$